

# Mechanism of Calponin Stabilization of Cross-Linked Actin Networks

Mikkel Herholdt Jensen,<sup>†‡</sup> Eliza J. Morris,<sup>‡</sup> Cynthia M. Gallant,<sup>§</sup> Kathleen G. Morgan,<sup>§</sup> David A. Weitz,<sup>‡</sup> and Jeffrey R. Moore<sup>†\*</sup>

<sup>†</sup>Department of Physiology and Biophysics, Boston University, Boston, Massachusetts; <sup>‡</sup>School of Engineering and Applied Sciences, Harvard University, Cambridge, Massachusetts; and <sup>§</sup>Department of Health Sciences, Boston University, Boston, Massachusetts

**ABSTRACT** The actin-binding protein calponin has been previously implicated in actin cytoskeletal regulation and is thought to act as an actin stabilizer, but the mechanism of its function is poorly understood. To investigate this underlying physical mechanism, we studied an *in vitro* model system of cross-linked actin using bulk rheology. Networks with basic calponin exhibited a delayed onset of strain stiffening (10.0% without calponin, 14.9% with calponin) and were able to withstand a higher maximal strain before failing (35% without calponin, 56% with calponin). Using fluorescence microscopy to study the mechanics of single actin filaments, we found that calponin increased the flexibility of actin filaments, evident as a decrease in persistence length from 17.6  $\mu\text{m}$  without to 7.7  $\mu\text{m}$  with calponin. Our data are consistent with current models of affine strain behavior in semiflexible polymer networks, and suggest that calponin stabilization of actin networks can be explained purely by changes in single-filament mechanics. We propose a model in which calponin stabilizes actin networks against shear through a reduction of persistence length of individual filaments.

## INTRODUCTION

Actin is a highly ubiquitous, highly conserved protein abundant in nearly all eukaryotic cells. It acts as a highly dynamic mechanical component of the cell and is essential to many processes, such as cell adhesion, mechanosensing and mechanotransduction, cell motility, and the determination of cell shape and stiffness (1–4). In the cell, the dynamics and mechanics of the actin cytoskeleton are tightly regulated by upwards of 60 known actin-binding proteins, which makes for a highly complex system with several levels of emergent behavior (5–9).

The actin-binding protein calponin was discovered in smooth muscle (10,11) and was originally studied as a possible smooth-muscle regulator of actomyosin interactions (12–16). More recently, both the smooth-muscle isoform, basic calponin (h1CaP), and the nonmuscle isoforms, neutral and acidic calponins (h2CaP and h3CaP), have been implicated in the regulation of actin cytoskeletal mechanics and cellular mechanical signaling (17). Non-muscle calponins are known to be involved in actin stabilization (18), actin stress fiber formation and stability (19), mechanical stimulus response (20), cell migration, vascular development, and cytokinesis (21,22). Smooth-muscle calponin is known to respond to agonist-induced smooth-muscle contraction by relocating to the cortical actin (23), a translocation accompanied by changes in cytoskeletal remodeling (24). Basic calponin has also been shown to stabilize populations of actin filaments in smooth muscle cells (25). Upregulation of basic calponin in cultured

smooth-muscle tissue has also been found to increase the tensile strength of the tissue (26), an effect potentially important for proper function of smooth-muscle tissue under strain.

Despite growing evidence of the importance of calponin as a mechanical stabilizer of actin cytoskeletal structures, the underlying physical mechanism of calponin function remains unclear. To study the mechanical effects of calponin on actin networks, we used a model system of cross-linked reconstituted actin networks from human platelets. Similar actin model systems have previously been shown to mimic fundamental properties of the actin cytoskeleton with very few constituents, yielding insights into the physics of actin and semiflexible polymer networks (27–32). As a minimalistic system, a reconstituted calponin-actin network allows mechanical changes of the network to be directly related to the physical mechanisms underlying calponin function.

Using this model system, we found that actin networks with calponin failed at a higher maximum strain, suggesting that the direct mechanical interaction of calponin with actin is sufficient to stabilize actin networks. In addition, calponin delayed the onset of network strain stiffening, a change characteristic of networks with polymers of increased flexibility (30,33). Direct fluorescence imaging was used to investigate whether single-filament flexibility led to the changes seen in bulk rheology. We found that the addition of calponin reduced the persistence length of human platelet actin, consistent with previous work using rabbit skeletal muscle actin (34), resulting in the observed changes in bulk network behavior. By using previous models for isotropic actin networks under affine strain, we show that the reduced persistence length seen on the single-filament level is sufficient to explain the rheological behavior in bulk networks.

Submitted June 28, 2013, and accepted for publication December 23, 2013.

\*Correspondence: [jxmoore@bu.edu](mailto:jxmoore@bu.edu)

Mikkel Herholdt Jensen and Eliza J. Morris contributed equally to this work.

Editor: Gijsje Koenderink.

© 2014 by the Biophysical Society  
0006-3495/14/02/0793/8 \$2.00



Together, these data show that calponin alone can stabilize actin networks against external shear. We suggest a model in which the calponin-induced increased flexibility of single actin filaments leads to a more shear-resistant actin network. To our knowledge, this represents the first direct physical model for calponin stabilization of actin networks.

## MATERIALS AND METHODS

### Proteins

Basic calponin (h1CaP) from ferret was expressed as previously described (34,35). A pTYP2 vector with a C-terminal chitin binding domain was used to generate a bacterial expression vector for ferret h1CaP (IMPACT-CN System, New England Biolabs, Ipswich, MA). The ferret h1CaP was amplified by polymerase chain reaction using oligonucleotides 5'-gga att cca tat gat gtc ctc tgc tca c-3' and 5'-ctc gag ggc gga gtt ata gta gtt g-3' and pET30b(+)-h1CaP as the template. The calponin fragment was cloned into the vector by NdeI and XhoI restriction sites, and DNA sequencing was used to confirm the validity of the construct. *Escherichia Coli* BL21 cells were used as expression hosts. Cell pellets were resuspended in lysis buffer (20 mM Tris-HCl, pH 8.0, 500 mM NaCl, 1 mM EDTA, and 0.1% Triton X-100) and sonicated, after which the supernatant containing the expressed h1CaP protein was purified using chitin beads. After purification, the calponin was stored on ice at 4°C. To avoid potential artifacts of protein aging, all experiments with calponin were performed within 2 weeks of purification.

Actin, all of >99% purity, was purchased as lyophilized powder from Cytoskeleton (Cytoskeleton, Denver, CO) and stored at -80°C until use. Flexural rigidity experiments used unlabeled human platelet actin, a mixture of 85% nonmuscle  $\beta$ -actin and 15% nonmuscle  $\gamma$ -actin, and human platelet actin labeled with rhodamine on random surface lysine residues to a labeling ratio of 0.5 dyes/monomer. Bulk rheology experiments used unlabeled human platelet actin and rabbit skeletal muscle actin biotinylated on random surface lysine residues to a ratio of 1:1 biotin/monomer. Neutravidin was from Sigma Aldrich (St. Louis, MO).

### Network bulk rheology

All bulk rheology was done on an Ares-G2 stress-controlled rheometer (TA Instruments, New Castle, DE) using a parallel plate geometry with a 40-mm-diameter top plate. Both top and bottom geometries were custom made of roughened stainless steel. After initial calibration and rotational mapping, the rheometer geometries were cleaned before each sample with one volume of acetone, one volume of isopropanol, one volume of glassware dish soap, and three volumes of distilled water (10 mL each).

On the day before the experiment, lyophilized G-actin from human platelets and biotinylated rabbit skeletal muscle actin was resuspended to a concentration of 4 mg/mL (plain actin) or 0.1 mg/mL (biotinylated actin) in G-buffer (0.2 mM CaCl<sub>2</sub>, 0.2 mM ATP, 0.2 mM dithiothreitol (DTT), 0.005% NaN<sub>3</sub>, and 2 mM Tris-HCl, pH 8.0).

Cross-linked actin networks were formed by polymerizing actin to 0.5 mg/mL with a 1:100 ratio of biotinylated actin (final buffer conditions were 2 mM MgCl<sub>2</sub>, 0.2 mM CaCl<sub>2</sub>, 100 mM KCl, 0.5 mM ATP, 0.2 mM DTT, and 2 mM Tris-HCl, pH 7.5). Filaments were cross-linked by the addition of neutravidin in a twofold molar excess to biotinylated actin, concurrent with the addition of calponin, after which the proteins were mixed and immediately loaded onto the rheometer with a geometry gap size of 200  $\mu$ m. The sample was sealed at the edges using mineral oil (Sigma Aldrich) and left to further polymerize and form cross-links for 1 h at 25°C, during which the shear modulus was monitored by applying a 1 rad/s sinusoidal oscillation with a 0.5% strain amplitude. The network

was then subjected to a slow strain ramp with a strain rate of 0.25%/s until network failure occurred.

### Filament flexural rigidity

The flexural rigidity of actin filaments is quantified in terms of its persistence length,  $L_p$ . It is geometrically interpreted as the arc-length distance over which two segments of the polymer tend to be uncorrelated in their orientations, and can be expressed by the cosine correlation function as

$$\langle \cos[\theta(s) - \theta(0)] \rangle = e^{-\frac{s}{L_p}}. \quad (1)$$

Thus, a higher persistence length corresponds to a more rigid polymer.  $\theta(s)$  denotes the tangent angle of the filament at arc length  $s$ , and the angle brackets indicate a temporal average. Due to the semiflexible nature of actin, the cosine correlation function can be used directly to determine the persistence length of actin by fitting Eq. 1 to the parameterizations of  $\theta(s)$  from images of thermally fluctuating filaments (36–39).

Persistence-length measurements of human-platelet actin filaments were performed as previously described for rabbit skeletal muscle actin (34). Higher concentrations were used to compensate for the higher critical concentration of the nonmuscle actin isoform (40–42). Lyophilized unlabeled actin and rhodamine-labeled actin were resuspended in 0.2 mM CaCl<sub>2</sub>, 0.2 mM ATP, 10 mM DTT, and 5 mM Tris-HCl, pH 8.0. A portion of the rhodamine-labeled actin was then polymerized at room temperature at 0.8 mg/mL in 50 mM KCl, 2 mM MgCl<sub>2</sub>, 1 mM ATP, and 1 mM DTT. After 2 h, the actin was vortexed at low speed for 30 s to shear the actin into smaller filament seeds. These smaller filaments were then mixed with a fourfold excess of rhodamine G-actin to a final actin concentration of 1  $\mu$ M and left overnight at 4°C in final buffer conditions of 25 mM KCl, 25 mM imidazole, 1 mM EGTA, 4 mM MgCl<sub>2</sub>, 1 mM ATP, and 10 mM DTT.

On the day of the experiment, microscope slides and coverslips (Corning Glass, Corning, NY) were dipped and rinsed in 10 mg/mL bovine-serum-albumin (BSA) twice and left to dry under a dust cover. Polymerized actin and fivefold molar excess of calponin were mixed with unlabeled G-actin in an oxygen scavenger buffer (2 mM dextrose, 160 U glucose oxidase, 2 mM catalase, 10 mM DTT, 1 mM ATP, 100 mM KCl, 25 mM imidazole, 1 mM EGTA, and 4 mM MgCl<sub>2</sub>). The final concentrations of the fluorescence microscopy samples were 15 nM of labeled F-actin and 485 nM of unlabeled G-actin. The total actin concentration was chosen close to the barbed-end critical concentration to help stabilize the filaments from depolymerization during imaging without significantly adding to their length (34,37). After incubation at room temperature for 30 min, 3  $\mu$ L of the sample was deposited onto a BSA-coated microscope slide. A BSA-coated coverslip was gently set on top and compressed to form a narrow flow chamber. The sample was then heated to 30°C by an objective heater (Bioptechs, Butler, PA) and then imaged under epifluorescence illumination on an inverted Nikon Eclipse TE2000-U microscope with an oil immersion 1.30 NA objective (Nikon, Melville, NY). Forty to eighty images of thermally fluctuating filaments, typically 5–10  $\mu$ m in length, were captured 5 s apart using the Scion Image frame grabber software (Scion, Frederick, MD) and an ICCD camera (PTI IC 310B, Birmingham, NJ) to avoid excessive temporal correlation between frames (43,44). If any fluid flow was evident after sample preparation, imaging was delayed for a few minutes until the flow settled and the filament underwent no directional motion but stayed within a small region during imaging, consistent with thermal diffusive motion of actin filaments based on measured diffusion coefficients of F-actin (45).

Images of filaments were skeletonized in ImageJ (rsbweb.nih.gov/ij). After flattening the image, enhancing the contrast, and smoothing with a Gaussian blur with a standard deviation of 0.25  $\mu$ m, the image was magnified fivefold using a bicubic pixel interpolation, thresholded, and eroded to form a 1-pixel-wide filament skeleton. Tangent angles along

the skeleton were derived using a custom-written Matlab script (MathWorks, Natick, MA) connecting skeleton pixels 10 pixels (0.3–0.4  $\mu\text{m}$ ) apart, and the persistence length was extracted for each movie by fitting Eq. 1 to the data.

## RESULTS

### Basic calponin increased the maximum strain of actin networks

Since polymerizing *in vitro* actin networks percolate into a nonthermal equilibrium state (46), we found that the exact procedure for the mixing of proteins before rheology measurements was critical to forming reproducible networks. We therefore mixed the G-actin with biotinylated G-actin and induced polymerization for exactly 60 s before adding neutravidin and calponin. This ensured proper incorporation of the biotinylated actin into F-actin filaments before cross-linking was initiated, and helped avoid inhomogeneities in the sample. Neutravidin and calponin were mixed into the F-actin over 10 s by slow pipetting, after which the sample was loaded onto the rheometer to polymerize and percolate further.

Once formed, cross-linked actin networks were strained at a constant rate using bulk rheology to determine the effects of basic calponin on the mechanical properties of actin networks. At every strain during the strain ramp, the mechanical response was quantified in terms of the corresponding network stress (Fig. 1 A). For the concentrations of actin and cross-linkers used in this work, the strained networks exhibited three distinct mechanical regimes: linear, strain-stiffening, and failure (Fig. 1 B). After the initial linear regime, during which the differential elastic modulus was largely constant, the networks strain stiffened, indicating full network percolation (28). The samples eventually entered a failure regime, characterized by a decreasing differential modulus, before reaching a yield stress and strain of  $\sigma_{max}$  and  $\gamma_{max}$ .

Both with and without calponin, the cross-linked actin networks formed a predominantly elastic but soft gel, exhibiting a linear shear modulus of a few Pascal, a fraction of that of Jell-O. Actin networks with a twofold molar excess of calponin had a slightly lower linear elastic modulus ( $G' = 3.2 \pm 0.3$  Pa without calponin compared to  $2.8 \pm 0.4$  Pa with calponin) and yielded on average at a 60% higher strain when compared to undecorated actin networks (Fig. 2), with the mean yield strain increasing from  $35 \pm 1.4\%$  to  $56 \pm 2.8\%$  ( $p < 0.001$ ). The mean yield stress demonstrated a much higher degree of variability, and although  $\sigma_{max}$  increased 150% in networks with calponin, from  $1.9 \pm 0.2$  Pa to  $4.8 \pm 1.6$  Pa, this difference was not statistically significant ( $p = 0.13$ ). Despite these large variations in yield stress (Fig. 2 A), samples were remarkably self-similar when normalized to their mean values (Fig. 2 B), indicating fundamentally distinct stress-strain behavior between samples with and without calponin.

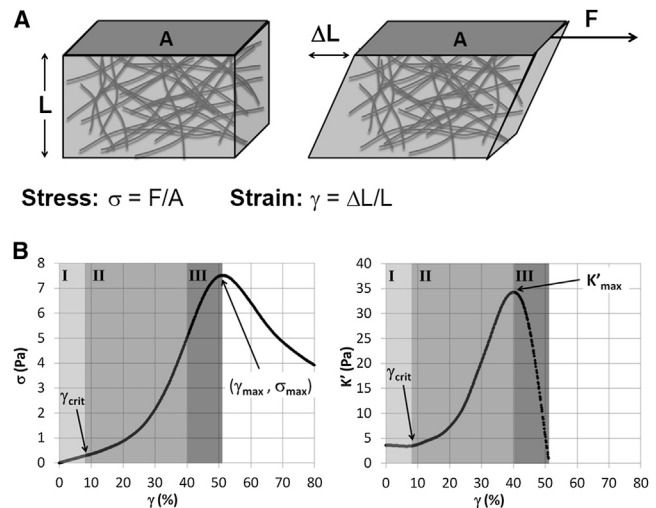


FIGURE 1 Shear bulk rheology was used to probe the mechanical properties of actin networks. (A) Cartoon representation of a sample undergoing a shear deformation. The shear stress is the force ( $F$ ) per cross-sectional area of the sample, whereas the strain is the unitless shear displacement of the sample. (B) Representative stress-strain curve and differential elastic modulus,  $K' = \partial\sigma/\partial\gamma$  (the slope of the stress-strain curve), of a fully percolated actin network with a twofold molar excess of calponin. Under a shear deformation, the network exhibited three mechanical regimes. In the linear regime (I), the network responded as a linear spring with a constant differential elastic modulus. Upon reaching a critical strain,  $\gamma_{crit}$ , the elasticity of the material increased with strain, termed strain stiffening (II). After reaching a maximum elastic modulus, the network entered a failure regime (III) and strain weakened as it began breaking, eventually reaching a yield stress,  $\sigma_{max}$ , and yield strain,  $\gamma_{max}$ .

### Networks with calponin exhibited a delayed onset of strain stiffening

The physical mechanisms underlying the increased maximum strain of calponin-actin networks were investigated by comparing stress-strain curves of cross-linked actin networks with and without basic calponin. Differences in the stress-strain behavior were visualized by normalizing stress-strain curves to the mean values of  $\sigma_{max}$  and  $\gamma_{max}$ . This normalization showed that calponin delayed the onset of strain stiffening and prolonged the relative time spent in the linear regime (Fig. 3, A and B). To quantify this effect, we calculated the onset of strain stiffening,  $\gamma_{crit}$ , defined as the intersection of the linear elastic modulus and the power-law extrapolation of the nonlinear regime of the differential elastic modulus,  $K' = \partial\sigma/\partial\gamma$  (Fig. 3 C). The  $\gamma_{crit}$  in networks with a twofold molar excess of calponin increased by  $\sim 50\%$ , from  $10.0 \pm 0.6\%$  to  $14.9 \pm 1.0\%$  ( $p < 0.01$ ; Fig. 3 D).

### Networks showed a gradual change in rheology with subsaturating amounts of calponin

To establish whether the rheological changes seen in actin networks fully decorated with calponin were caused

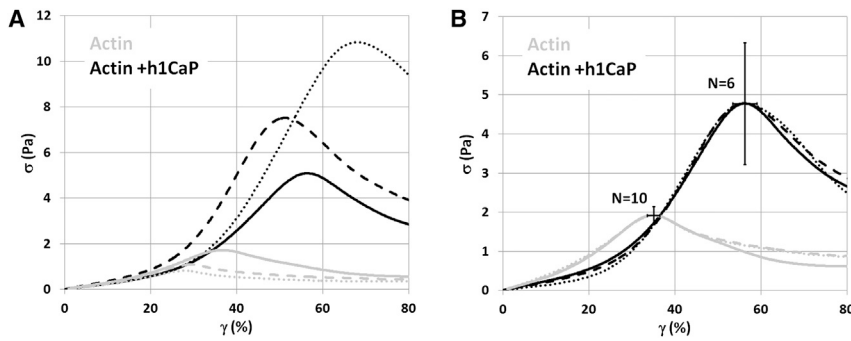


**FIGURE 2** Calponin increased the maximum strain of cross-linked actin networks. (A) Three representative bulk rheology stress-strain curves for 0.5 mg/mL actin cross-linked with a 1:100 molar ratio of biotin-actin without (gray lines) or with (black lines) a twofold molar excess of basic calponin. (B) Normalizing the stress-strain curves to their respective mean stresses and strains collapsed the curves and revealed a high degree of similarity between samples either with or without calponin. The mean yield strain increased from  $35 \pm 1.4\%$  to  $56 \pm 2.8\%$  ( $p < 0.001$ ). The increase in mean yield stress, from  $1.9 \pm 0.2$  Pa to  $4.8 \pm 1.6$  Pa, was not statistically significant ( $p = 0.13$ ). Error bars represent the mean  $\pm$  SE.

by drastic alterations of the filaments only occurring at high calponin concentrations, we conducted bulk rheology measurements in networks with subsaturating amounts of calponin (Fig. 4). As observed at fully saturating levels of calponin (Fig. 2), the yield stress exhibited a large degree of variability between samples. However, a gradual increase was seen in both the yield strain (Fig. 4 A) and the onset of strain stiffening (Fig. 4 B) as the calponin concentration was increased. These continuous changes were similar to those seen at complete calponin decoration, suggesting that the observed rheological effects were a proportional response to the amount of calponin bound to actin, rather than a more drastic filament rearrangement occurring only at high concentrations of calponin.

### Calponin made single filaments more flexible

To relate the network behavior to the mechanical changes induced by calponin in individual actin filaments, we

quantified the persistence length of F-actin with and without a fivefold molar excess of basic calponin. Fluorescently labeled actin filaments freely fluctuating in two dimensions were imaged over time, skeletonized, and parameterized in terms of an angle,  $\theta$ , and the filament arc length,  $s$  (Fig. 5, A and B). The persistence length was extracted from the cosine correlation function for each filament (Fig. 5 C). Filaments incubated with a fivefold molar excess of basic calponin showed an  $\sim 50\%$  reduction in persistence length, from  $17.6 \pm 0.7 \mu\text{m}$  to  $7.7 \pm 0.6 \mu\text{m}$  ( $p < 0.001$ ).

## DISCUSSION

In a complex system with many layers of emergent behavior, as, for example, in living cells or tissue, it is difficult to determine whether a single protein is sufficient to affect actin cytoskeletal structures, or whether it acts in tandem with other actin-binding proteins or cellular components. As such, although calponin has been linked to

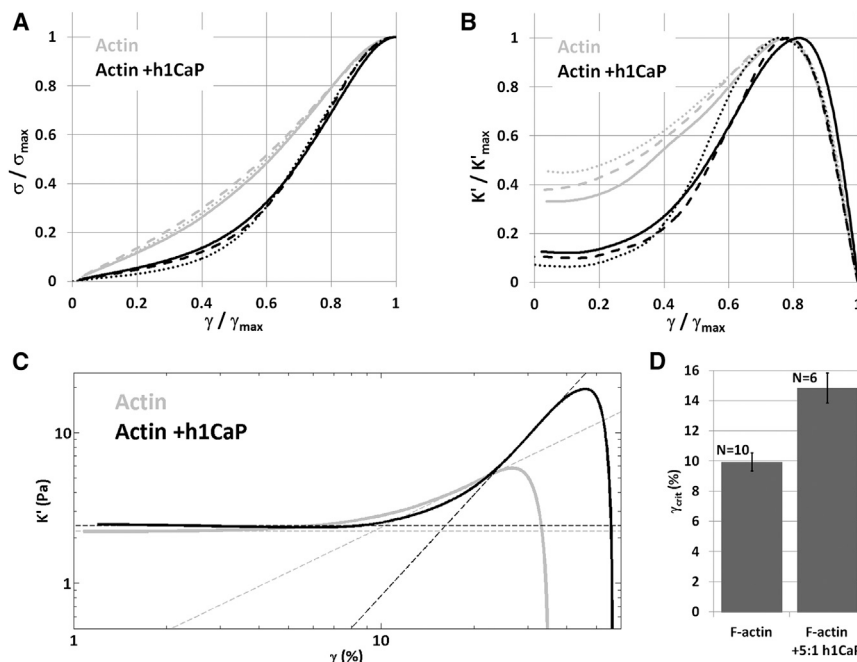


**FIGURE 3** Calponin delayed the onset of strain stiffening in cross-linked actin networks. (A) The bulk rheology stress-strain curves from Fig. 2 with (black lines) or without (gray lines) a twofold molar excess of calponin, normalized by the yield stress,  $\sigma_{max}$ , and yield strain,  $\gamma_{max}$ , of each curve. (B) The differential elastic modulus,  $K'$ , of the stress-strain curves shown in A, normalized by  $\gamma_{max}$  and  $K'$  of each curve. Samples with and without calponin were similar, with the exception of a delayed onset of strain stiffening in samples with calponin. (C) The onset of strain stiffening,  $\gamma_{crit}$ , was defined as the strain at which the linear elastic modulus and the power-law fit to the stress-strain curve in the nonlinear stiffening regime intersected (dashed lines). Shown are two stress-strain curves for samples with (black) and without (gray) a twofold molar excess of basic calponin. (D) Onset of strain stiffening was increased from  $10.0 \pm 0.6\%$  without calponin to  $14.9 \pm 1.0\%$  with calponin ( $p < 0.01$ ). Error bars represent the mean  $\pm$  SE.



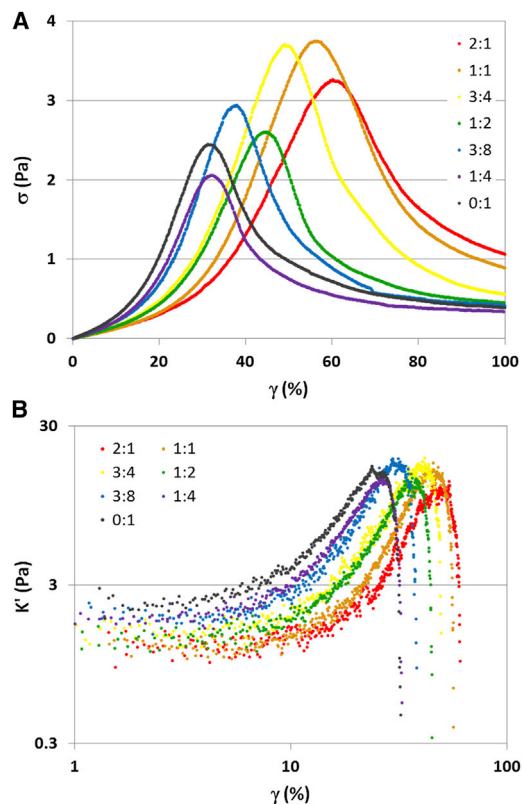


FIGURE 4 Network rheological behavior was gradually altered with increasing calponin concentration. Bulk rheology stress-strain curves of cross-linked actin networks with calponin/actin molar ratios ranging from 0:1 to 2:1 revealed a gradual shift in yield strain,  $\gamma_{max}$  (A), and onset of strain stiffening,  $\gamma_{crit}$  (B), as the concentration of calponin was increased. These changes were evident even at subsaturating concentrations of calponin, suggesting that actin networks partially decorated with calponin exhibit changes similar to, but less pronounced than, those seen in fully decorated networks.

the regulation and stabilization of the actin cytoskeleton through cell and tissue studies, the underlying physical mechanisms remain unclear. To address this, we used an experimental model system of reconstituted cross-linked actin from human platelets to study the direct mechanical effects of calponin on actin networks. Such systems have previously been shown to capture essential mechanical properties of living cell systems, but with a drastically reduced number of variables (27–32). Employing only the most fundamental material components, cross-linked actin and calponin, this model system is ideally suited to address the physical mechanisms of the mechanical effects of calponin on actin networks.

The mechanical effect of calponin on the actin networks was probed using bulk rheology. As entangled actin exhibits neither strain stiffening nor subsequent failure, but rather weakens and flows under strain, we focused on cross-linked actin networks to characterize the effects of calponin on network mechanics. Biotin-neutravidin cross-linked actin networks are rheologically similar to

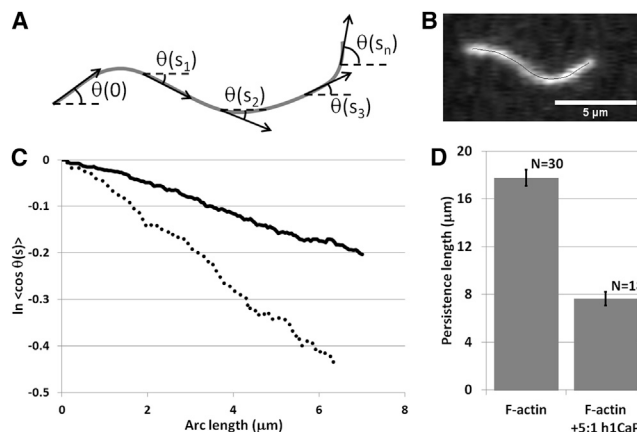


FIGURE 5 Calponin reduced the persistence length of single actin filaments. (A) Thermally fluctuating actin filaments were imaged and parameterized in terms of an angle,  $\theta$ , and the filament arc length,  $s$ . (B) Representative raw image of a fluorescently labeled actin filament. Overlaid is the corresponding filament skeleton backbone used for parameterization and analysis. (C) The cosine correlation function was used to determine the persistence length. Shown are data from movies of two single actin filaments with (dotted line) and without (solid line) a fivefold molar excess of basic calponin. The persistence lengths were derived from the slope of the curves (Eq. 1). (D) Calponin reduced the persistence length of actin from  $17.6 \pm 0.7 \mu\text{m}$  to  $7.7 \pm 0.6 \mu\text{m}$  ( $p < 0.001$ ). Error bars represent the mean  $\pm$  SE.

in vitro actin networks cross-linked with static biological cross-linkers, like scruin (28) or heavy meromyosin in the absence of ATP (30), and thus, this network was chosen as an experimental system over dynamically binding biological cross-linkers to maintain a dynamically arrested isotropic network during the course of the experiment. The actin concentration and the 1:100 molar ratio of biotin-actin to plain actin were chosen to ensure that samples were fully percolated and exhibited strain stiffening (28). Under these conditions, for a number of reasons, the maximal strain,  $\gamma_{max}$ , and maximal stress,  $\sigma_{max}$ , was interpreted as a network failure, and not bulk detachment of the network from the rheometer geometries. First, the transition to failure was gradual even at the very low strain rate used in this experiment, which is uncharacteristic of catastrophic and abrupt surface detachments. Second, similar in vitro actin networks have been strained to carry shear loads an order of magnitude or more beyond those applied here, without surface detachment from identical rheometer geometries (27). Third, it has been shown previously that the maximum stress scales roughly linearly with the actin concentration present, suggesting that the failure is due to individual actin filaments in the network rather than to bulk surface detachment (29,47). Although a reduction in cross-linking density or a lowering of polymer concentration would both lead to a higher yield strain of the network, both are accompanied by a lower yield stress as well (Fig. S1 in the Supporting Material), contrary to what was observed in actin networks with

calponin (Fig. 2). Thus, our data are not consistent with a reduction in cross-linking density or a dilution of F-actin by calponin, and they demonstrate that calponin alone is sufficient to strengthen an in vitro actin network structure without additional actin-binding proteins or other cellular components present.

To better understand the mechanism by which calponin stabilized the actin networks, we examined the strain-stiffening behavior of the actin networks with and without calponin. The normalization and subsequent collapse of the stress-strain curves for each experimental condition (Fig. 2 and Fig. 3, A and B) highlighted distinct differences in the stress-strain response of plain actin networks compared to calponin-actin networks and demonstrated that calponin induced a change not only in the maximum strain but also in the overall stress-strain behavior of the networks by delaying the onset of strain stiffening (Fig. 3). The delay in strain stiffening and the increase in yield strain were also observed in bulk rheology experiments with subsaturating concentrations of calponin (Fig. 4), suggesting that subsaturating amounts of calponin are sufficient to elicit a mechanical change in cytoskeletal actin networks. Furthermore, increasing the calponin concentration resulted in a continuous change toward higher yield strains and delayed stiffening, suggesting that the mechanical changes observed at full decoration were mechanically similar to those at lower calponin concentrations rather than a drastic discrete change in filament mechanics occurring only at high calponin concentrations.

Given the strain-stiffening behavior observed at the concentrations of cross-linkers and actin used here, actin networks can be assumed to behave in an affine manner under strain, with elasticity originating from the entropic nature of the individual polymers (28,33). In an affine network of entropic springs, both the onset of strain stiffening,  $\gamma_{crit}$ , and the eventual yield strain,  $\gamma_{max}$ , are inversely proportional to the persistence length of the polymers making up the network. Thermal fluctuations within semi-flexible polymer networks reduce the equilibrium end-to-end length of individual polymer segments. The more flexible the polymers, the greater the thermal undulations become. As the flexibility of individual actin polymers is increased, there are more thermal undulations to pull out, and because of this extra slack, a network of more flexible polymers will stiffen at a higher strain and withstand higher external strains before failing (30,33). In our experiments, the 60% increase in  $\gamma_{max}$  with twofold molar excess of calponin (Fig. 2) was accompanied by a 50% increase in  $\gamma_{crit}$  (Fig. 3). We therefore hypothesized that the increase in maximum strain observed in our bulk rheology data resulted from a reduction in the persistence length of individual actin filaments.

To test this hypothesis, we directly measured the persistence length of actin filaments from human platelets by fluorescence microscopy (Fig. 5). To avoid any effects on

persistence length, all measurements in this work were done using rhodamine-labeled actin rather than phalloidin. We measured a persistence length of 17.6  $\mu\text{m}$  for human platelet actin, within the range of 6–19  $\mu\text{m}$  measured by others using rabbit skeletal actin without actin-binding proteins or phalloidin (34,37,38,48,49). The introduction of calponin reduced the actin persistence length roughly twofold, to 7.7  $\mu\text{m}$ . This reduction is larger than that previously observed with basic calponin and rabbit skeletal muscle actin (34), likely due to differences in protein concentrations. Although similar calponin/actin ratios were used, the higher protein concentrations used in this work would lead to more complete decoration of the actin filaments due to the concentration-dependent binding rate of calponin, consistent with previously reported dissociation constants of actin-calponin (50,51). However, it is also possible that the larger decrease in persistence length could arise from differences between actin isoforms. We therefore restrict ourselves to using only human platelet nonmuscle actin for all experiments in this work, as it is more physiologically relevant to the smooth-muscle actin-binding protein basic calponin.

Previous work has linked bulk rheological changes to the mechanical properties of individual filaments within the framework of the affine network model (52). Within this framework, the polymer persistence length is directly related to the bulk modulus,  $G'$ , the polymer density,  $\rho$ , and the onset of strain stiffening as

$$L_p \sim \rho k_B T \frac{(G')^2}{\sigma_{crit}^3}. \quad (2)$$

In other words, the mechanical properties observed in bulk rheology can be directly related to changes in the flexibility of individual filaments, since this flexibility is what determines the elastic properties of the entire network. Since  $G' = \sigma/\gamma$ , Eq. 2 can be rewritten as

$$L_p \sim \rho k_B T \frac{1}{G' \gamma_{crit}^3}. \quad (3)$$

Thus, our bulk rheology data can be used to predict underlying persistence-length changes of individual actin polymers upon the addition of calponin. Using the measured values for  $G'$  (3.2  $\pm$  0.3 Pa for plain actin networks versus 2.8  $\pm$  0.4 Pa for calponin-decorated actin networks) and  $\gamma_{crit}$  (10.0  $\pm$  0.6% for plain actin networks versus 14.9  $\pm$  1.0% for calponin-decorated actin networks; Fig. 3), we estimate the persistence length with twofold molar excess of calponin to be 35% of that of plain actin in the bulk rheology. This value agrees well with the directly observed reduction in persistence length by fluorescence microscopy in the presence of a fivefold molar calponin excess, from 17.6  $\mu\text{m}$  to 7.7  $\mu\text{m}$ , or 43% of the value in the absence of calponin (Fig. 5). Based on reported dissociation constants

for calponin and actin (51), the chosen molar ratios correspond to 80–90% decoration in both bulk and single-filament experiments, with the higher molar ratio in the single-filament studies offsetting the lower overall protein concentration.

This observed reduction in single-filament persistence length matches the prediction from bulk rheology, suggesting that the reduced persistence length is sufficient to explain the increases in  $\gamma_{max}$  and  $\gamma_{crit}$  within the framework of the previously proposed affine network model (30,33,52). This suggests a simple mechanism through which calponin mechanically stabilizes actin networks under external strain by making individual actin filaments more flexible. The stabilization of actin networks by calponin is explained in terms of a single parameter, the actin flexural rigidity. Although the exact function of calponin in the cell is likely to depend on multiple physical and chemical variables, our in vitro model system yields a fundamental, first-order explanation for calponin stabilization of actin structures that qualitatively captures the effects of calponin observed in tissues and cells.

## SUPPORTING MATERIAL

One figure is available at [http://www.biophysj.org/biophysj/supplemental/S0006-3495\(14\)00062-9](http://www.biophysj.org/biophysj/supplemental/S0006-3495(14)00062-9).

M.H.J. and E.J.M. thank Prof. Frederick C. MacKintosh for helpful discussions.

This work was supported by Program Project Grant HL86655 from the National Institutes of Health, and by the National Science Foundation (grants DMR-0820484 and DMR-1310266).

## REFERENCES

- Cooper, J. A. 1991. The role of actin polymerization in cell motility. *Annu. Rev. Physiol.* 53:585–605.
- Janmey, P. A. 1998. The cytoskeleton and cell signaling: component localization and mechanical coupling. *Physiol. Rev.* 78:763–781.
- Katsumi, A., A. W. Orr, ..., M. A. Schwartz. 2004. Integrins in mechanotransduction. *J. Biol. Chem.* 279:12001–12004.
- Small, J. V., and G. P. Resch. 2005. The comings and goings of actin: coupling protrusion and retraction in cell motility. *Curr. Opin. Cell Biol.* 17:517–523.
- Ayscough, K. R. 1998. In vivo functions of actin-binding proteins. *Curr. Opin. Cell Biol.* 10:102–111.
- McGough, A. 1998. F-actin-binding proteins. *Curr. Opin. Struct. Biol.* 8:166–176.
- Pollard, T. D., and G. G. Borisy. 2003. Cellular motility driven by assembly and disassembly of actin filaments. *Cell.* 112:453–465.
- Dominguez, R. 2004. Actin-binding proteins—a unifying hypothesis. *Trends Biochem. Sci.* 29:572–578.
- Paavilainen, V. O., E. Bertling, ..., P. Lappalainen. 2004. Regulation of cytoskeletal dynamics by actin-monomer-binding proteins. *Trends Cell Biol.* 14:386–394.
- Lehman, W., and B. Kaminer. 1984. Identification of a thin filament linked-35,000 dalton protein in vertebrate smooth-muscle. 1984 *Biophysical Society Meeting Abstracts*. Supplement, 109a. Abstract.
- Takahashi, K., K. Hiwada, and T. Kokubu. 1986. Isolation and characterization of a 34,000-dalton calmodulin- and F-actin-binding protein from chicken gizzard smooth muscle. *Biochem. Biophys. Res. Commun.* 141:20–26.
- Winder, S. J., B. G. Allen, ..., M. P. Walsh. 1998. Regulation of smooth muscle actin-myosin interaction and force by calponin. *Acta Physiol. Scand.* 164:415–426.
- Winder, S. J., and M. P. Walsh. 1990. Smooth muscle calponin. Inhibition of actomyosin MgATPase and regulation by phosphorylation. *J. Biol. Chem.* 265:10148–10155.
- Shirinsky, V. P., K. G. Biryukov, ..., J. R. Sellers. 1992. Inhibition of the relative movement of actin and myosin by caldesmon and calponin. *J. Biol. Chem.* 267:15886–15892.
- Takahashi, K., M. Abe, ..., T. Kokubu. 1988. A novel troponin T-like protein (calponin) in vascular smooth muscle: interaction with tropomyosin paracrystals. *J. Hypertens. Suppl.* 6:S40–S43.
- Takahashi, K., K. Hiwada, and T. Kokubu. 1988. Vascular smooth muscle calponin. A novel troponin T-like protein. *Hypertension.* 11:620–626.
- Rozenblum, G. T., and M. Gimona. 2008. Calponins: adaptable modular regulators of the actin cytoskeleton. *Int. J. Biochem. Cell Biol.* 40:1990–1995.
- Shibukawa, Y., N. Yamazaki, ..., Y. Wada. 2010. Calponin 3 regulates actin cytoskeleton rearrangement in trophoblastic cell fusion. *Mol. Biol. Cell.* 21:3973–3984.
- Daimon, E., Y. Shibukawa, and Y. Wada. 2013. Calponin 3 regulates stress fiber formation in dermal fibroblasts during wound healing. *Arch. Dermatol. Res.* 305:571–584.
- Hossain, M. M., J. F. Crish, ..., J. P. Jin. 2005. h2-Calponin is regulated by mechanical tension and modifies the function of actin cytoskeleton. *J. Biol. Chem.* 280:42442–42453.
- Tang, J., G. Hu, ..., V. P. Sukhatme. 2006. A critical role for calponin 2 in vascular development. *J. Biol. Chem.* 281:6664–6672.
- Hossain, M. M., D. Y. Hwang, ..., J. P. Jin. 2003. Developmentally regulated expression of calponin isoforms and the effect of h2-calponin on cell proliferation. *Am. J. Physiol. Cell Physiol.* 284:C156–C167.
- Parker, C. A., K. Takahashi, ..., K. G. Morgan. 1994. Agonist-induced redistribution of calponin in contractile vascular smooth muscle cells. *Am. J. Physiol.* 267:C1262–C1270.
- Kim, H. R., C. Gallant, ..., K. G. Morgan. 2008. Cytoskeletal remodeling in differentiated vascular smooth muscle is actin isoform dependent and stimulus dependent. *Am. J. Physiol. Cell Physiol.* 295:C768–C778.
- Gimona, M., I. Kaverina, ..., G. Burgstaller. 2003. Calponin repeats regulate actin filament stability and formation of podosomes in smooth muscle cells. *Mol. Biol. Cell.* 14:2482–2491.
- Arrigoni, C., D. Camozzi, ..., A. Remuzzi. 2006. The effect of sodium ascorbate on the mechanical properties of hyaluronan-based vascular constructs. *Biomaterials.* 27:623–630.
- Gardel, M. L., F. Nakamura, ..., D. A. Weitz. 2006. Prestressed F-actin networks cross-linked by hinged filamins replicate mechanical properties of cells. *Proc. Natl. Acad. Sci. USA.* 103:1762–1767.
- Gardel, M. L., J. H. Shin, ..., D. A. Weitz. 2004. Elastic behavior of cross-linked and bundled actin networks. *Science.* 304:1301–1305.
- Gardel, M. L., K. E. Kasza, ..., D. A. Weitz. 2008. Chapter 19: Mechanical response of cytoskeletal networks. *Methods Cell Biol.* 89:487–519.
- Tharman, R., M. M. Claessens, and A. R. Bausch. 2007. Viscoelasticity of isotropically cross-linked actin networks. *Phys. Rev. Lett.* 98:088103.
- Kasza, K. E., G. H. Koenderink, ..., D. A. Weitz. 2009. Nonlinear elasticity of stiff biopolymers connected by flexible linkers. *Phys. Rev. E Stat. Nonlin. Soft Matter Phys.* 79:041928.
- Kasza, K. E., A. C. Rowat, ..., D. A. Weitz. 2007. The cell as a material. *Curr. Opin. Cell Biol.* 19:101–107.

33. MacKintosh, F. C., J. Käs, and P. A. Janmey. 1995. Elasticity of semiflexible biopolymer networks. *Phys. Rev. Lett.* 75:4425–4428.
34. Jensen, M. H., J. Watt, ..., J. R. Moore. 2012. Effects of basic calponin on the flexural mechanics and stability of F-actin. *Cytoskeleton (Hoboken)*. 69:49–58.
35. Appel, S., P. G. Allen, ..., K. G. Morgan. 2010. h3/Acidic calponin: an actin-binding protein that controls extracellular signal-regulated kinase 1/2 activity in nonmuscle cells. *Mol. Biol. Cell*. 21:1409–1422.
36. Ott, A., M. Magnasco, ..., A. Libchaber. 1993. Measurement of the persistence length of polymerized actin using fluorescence microscopy. *Phys. Rev. E Stat. Phys. Plasmas Fluids Relat. Interdiscip. Topics*. 48:R1642–R1645.
37. Isambert, H., P. Venier, ..., M. F. Carrier. 1995. Flexibility of actin filaments derived from thermal fluctuations. Effect of bound nucleotide, phalloidin, and muscle regulatory proteins. *J. Biol. Chem.* 270:11437–11444.
38. Koster, S., D. Steinhauser, and T. Pfohl. 2005. Brownian motion of actin filaments in confining microchannels. *J. Phys. Condens. Matter*. 17:S4091–S4104.
39. McCullough, B. R., L. Blanchoin, ..., E. M. De la Cruz. 2008. Cofilin increases the bending flexibility of actin filaments: implications for severing and cell mechanics. *J. Mol. Biol.* 381:550–558.
40. Gordon, D. J., J. L. Boyer, and E. D. Korn. 1977. Comparative biochemistry of non-muscle actins. *J. Biol. Chem.* 252:8300–8309.
41. Rubenstein, P. A. 1990. The functional importance of multiple actin isoforms. *BioEssays*. 12:309–315.
42. Herman, I. M. 1993. Actin isoforms. *Curr. Opin. Cell Biol.* 5:48–55.
43. Gittes, F., B. Mickey, ..., J. Howard. 1993. Flexural rigidity of microtubules and actin filaments measured from thermal fluctuations in shape. *J. Cell Biol.* 120:923–934.
44. Brangwynne, C. P., G. H. Koenderink, ..., D. A. Weitz. 2007. Bending dynamics of fluctuating biopolymers probed by automated high-resolution filament tracking. *Biophys. J.* 93:346–359.
45. Li, G. L., and J. X. Tang. 2004. Diffusion of actin filaments within a thin layer between two walls. *Phys. Rev. E Stat. Nonlin. Soft Matter Phys.* 69:061921.
46. Falzone, T. T., M. Lenz, ..., M. L. Gardel. 2012. Assembly kinetics determine the architecture of  $\alpha$ -actinin crosslinked F-actin networks. *Nat. Commun.* 3:861.
47. Gardel, M. L., J. H. Shin, ..., D. A. Weitz. 2004. Scaling of F-actin network rheology to probe single filament elasticity and dynamics. *Phys. Rev. Lett.* 93:188102.
48. Takebayashi, T., Y. Morita, and F. Oosawa. 1977. Electronmicroscopic investigation of the flexibility of F-actin. *Biochim. Biophys. Acta*. 492:357–363.
49. Greenberg, M. J., C. L. Wang, ..., J. R. Moore. 2008. Modulation of actin mechanics by caldesmon and tropomyosin. *Cell Motil. Cytoskeleton*. 65:156–164.
50. Lu, F. W., M. V. Freedman, and J. M. Chalovich. 1995. Characterization of calponin binding to actin. *Biochemistry*. 34:11864–11871.
51. Ferjani, I., A. Fattoum, ..., C. Roustan. 2006. Calponin binds G-actin and F-actin with similar affinity. *FEBS Lett.* 580:4801–4806.
52. Lin, Y. C., N. Y. Yao, ..., D. A. Weitz. 2010. Origins of elasticity in intermediate filament networks. *Phys. Rev. Lett.* 104:058101.



## **Supporting Material**

### **Mechanism of calponin stabilization of crosslinked actin networks**

Mikkel Herholdt Jensen, Eliza J. Morris, Cynthia M. Gallant, Kathleen G. Morgan,  
David A. Weitz, Jeffrey R. Moore

Corresponding author:

Jeffrey R. Moore  
Boston University School of Medicine  
Department of Physiology and Biophysics  
72 East Concord Street  
Boston, MA 02118  
phone: 617-638-4251  
fax: 617-638-4273  
jxmoore@bu.edu

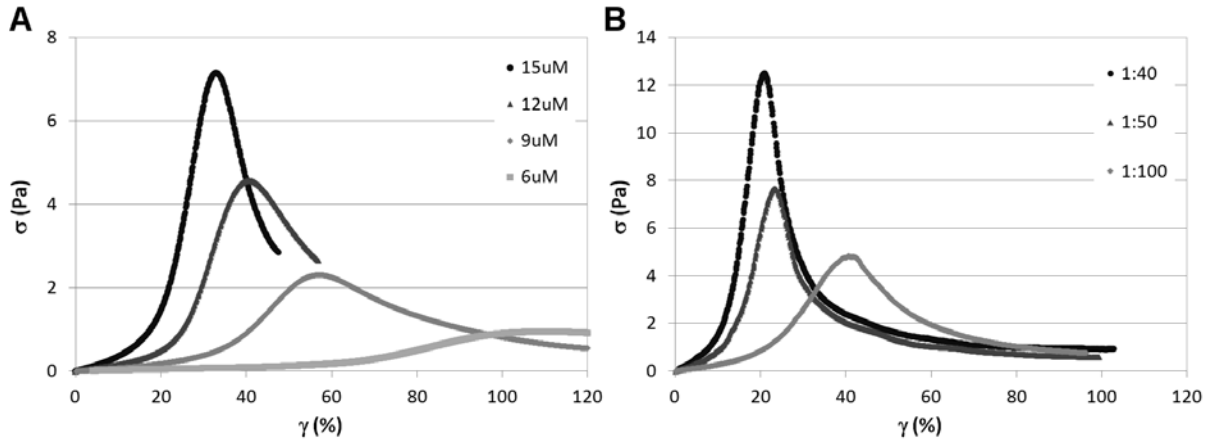


**Figure S1:** Effects of actin concentration and crosslinking density on network rheology. Crosslinked actin networks with a constant ratio of biotinylated actin to plain actin of 1:100 and variable actin concentrations (A), and a constant actin concentration of 15  $\mu$ M with various crosslinking densities (B) were polymerized and strained as described in the Materials and Methods. The maximal network strain,  $\gamma_{max}$ , is increased by either lowering the actin concentration or the crosslinking density; however, in both cases the maximal stress,  $\sigma_{max}$ , is decreased, contrary to what is seen in actin networks with calponin.